binding pocket (Fig. 3C).

To span the distance of 25 Å between the two binding pockets would require about seven residues. Sites of acetylation observed on H4 in vivo (K5, K8, K12, and K16) in active euchromatin (*15*) are consistent with this spacing. We performed further binding assays to define which sites of acetylation are important for the $TAF_{II}250$-DBD–H4 interaction. Peptides containing acetyllysine at K16, at K8/K16, and at K5/K12 were synthesized. The ITC measurements (Fig. 1) detected no significant binding for the unacetylated peptide, whereas multiple acetylation of H4 tails at lysine residues K5/K12, K8/K16, or K5/K8/K12/K16 dramatically enhanced binding. The K5/K12 peptide bound most tightly (K_d = 1.4 ± 0.3 μM; n = 1.05 ± 0.03), followed by the K5/K8/K12/K16 peptide (K_d = 5.3 ± 0.2 μM; n = 1.00 ± 0.01). Affinity for the fully acetylated K5/K8/K12/K16 peptide did not dramatically increase relative to K8/K16 (K_d = 5.6 ± 0.2 μM; n = 0.81 ± 0.01). However, singly acetylated peptides (K16) bound with reduced but still significant affinity (K_d ~ 40 μM) (Fig. 1). In contrast, a control peptide (KPGQPMYKGKKALRRQETVDAL) unrelated to histone tails acetylated at the NH_2-terminus and at K8 did not bind detectably to the bromodomains of $TAF_{II}250$. These data suggest that a single acetylated lysine within a peptide unrelated to histone H4 is not sufficient for high-affinity binding to the $TAF_{II}250$ bromodomains.

The ability of the double bromodomain of $TAF_{II}250$ to recognize histone H4 peptide tails containing transcriptionally relevant patterns of acetylation coupled with the striking distribution of charged residues on the protein fragment's surface hints at a new and unexpected role for $TAF_{II}250$. We suggest that these bromodomains may serve to target TFIID to promoters near or within regions of the chromosome that are nucleosome-bound. This would be in contrast to the notion that TFIID nucleates preinitiation complexes at nucleosome-free regions. Upon recognition of the acetylated tails of histone H4, the charged surfaces of the double bromodomain could potentially make nonspecific contacts with the nucleic acid on the basic side of the double bromodomain and contact the core histone molecules along the acidic surface. This notion provides an attractive possibility because TATA elements are often located near or within nucleosomes in vivo (*16*). A simplified scheme linking histone acetylation and core promoter recognition by TFIID (Fig. 4) might include recruitment by upstream activators of coactivator HAT activities such as CBP (*5*, *17*) or Gcn5 (*18*). These HATs could then acetylate appropriate lysine residues of the histones near core promoters thereby increasing affinity for TFIID. At this point there is no evidence that proteins containing both bromodomains and HAT domains concomitantly bind the same substrate. Thus the $TAF_{II}250$ HAT could potentially acetylate histones downstream of the core promoter, other basal transcription factors, or other as yet unidentified protein targets. This could set up a cascade of acetylation events opening the template and rendering it competent for activated transcription. This model would include a direct role for TFIID in targeting transcriptionally relevant patterns of acetylation within the histone tails and could provide a link between HAT activities and enhanced initiation through increased recruitment of TFIID to genes containing multiply acetylated histone tails.

References and Notes

1. G. Orphanides, T. Lagrange, D. Reinberg, *Genes Dev.* **10**, 2657 (1996).
2. J. A. Goodrich and R. Tjian, *Curr. Opin. Cell Biol.* **6**, 403 (1994).
3. S. K. Burley and R. G. Roeder, *Annu. Rev. Biochem.* **65**, 769 (1996); R. Tjian and T. Maniatis, *Cell* **77**, 5 (1994).
4. P. A. Wade and A. P. Wolffe, *Curr. Biol.* **7**, R82 (1997); M. J. Pazin and J. T. Kadonaga, *Cell* **89**, 325 (1997); P. A. Grant *et al.*, *Genes Dev.* **11**, 1640 (1997); V. V. Ogryzko, R. L. Schiltz, V. Russanova, B. H. Howard, Y. Nakatani, *Cell* **87**, 953 (1996); X. J. Yang, V. V. Ogryzko, J. Nishikawa, B. H. Howard, Y. Nakatani, *Nature* **382**, 319 (1996); T. E. Spencer *et al.*, *Nature* **389**, 194 (1997); H. Chen *et al.*, *Cell* **90**, 569 (1997); V. Allfrey, R. Faulkner, A. Mirsky, *Proc. Natl. Acad. Sci. U.S.A.* **51**, 786 (1964); J. E. Brownell and C. D. Allis, *Curr. Opin. Genet. Dev.* **6**, 176 (1996).
5. A. J. Bannister and T. Kouzarides, *Nature* **384**, 641 (1996).
6. C. A. Mizzen *et al.*, *Cell* **87**, 1261 (1996).
7. F. Jeanmougin, J. M. Wurtz, B. Le Douarin, P. Chambon, R. Losson, *Trends Biochem. Sci.* **22**, 151 (1997).
8. S. R. Haynes *et al.*, *Nucleic Acids Res.* **20**, 2603 (1992).
9. O. Matangkasombut, R. M. Buratowski, N. W. Swilling, S. Buratowski, *Genes Dev.* **14**, 951 (2000).
10. C. Dhalluin *et al.*, *Nature* **399**, 491 (1999).
11. C. A. Johnson, L. P. O'Neill, A. Mitchell, B. M. Turner, *Nucleic Acids. Res.* **26**, 994 (1998); M. H. Kuo *et al.*, *Nature* **383**, 269 (1996); S. Y. Roth and C. D. Allis, *Cell* **87**, 5 (1996); R. E. Sobel, R. G. Cook, C. A. Perry, A. T. Annunziato, C. D. Allis, *Proc. Natl. Acad. Sci. U.S.A.* **92**, 1237 (1995); B. M. Turner, *Cell* **75**, 5 (1993).
12. W. A. Hendrickson and C. M. Ogata, *Methods Enzymol.* **276**, 494 (1997).
13. G. Kleywegt, *Acta Crystallogr. D* **53**, 179 (1994).
14. Amino acid residues are abbreviated as follows: A, Ala; C, Cys; D, Asp; E, Glu; F, Phe; G, Gly; H, His; I, Ile; K, Lys; L, Leu; M, Met; N, Asn; P, Pro; Q, Gln; R, Arg; S, Ser; T, Thr; V, Val; W, Trp; Y, Tyr.
15. D. J. Clarke, L. P. O'Neill, B. M. Turner, *Biochem. J.* **294**, 557 (1993).
16. M. Grunstein, *Annu. Rev. Cell Biol.* **6**, 643 (1990).
17. V. V. Ogryzko *et al.*, *Cell* **94**, 35 (1998).
18. J. E. Brownell *et al.*, *Cell* **84**, 843 (1996).
19. S. C. Gill and P. H. von Hippel, *Anal. Biochem.* **182**, 319 (1989).
20. R. Koradi, M. Billeter, K. Wüthrich, *J. Mol. Graph.* **14**, 29, 51 (1996).
21. Collaborative Computational Project, *Acta. Crystallogr. D* **50**, 760 (1994).
22. J. Holton, unpublished program.
23. S. L. Roderick, unpublished program.
24. Z. Otwinowski, in *Isomorphous Replacement and Anomalous Scattering*, W. Wolf, P. R. Evans, A. G. W. Leslie, Eds. (The CCP4 Study Weekend, SERC Daresbury Laboratory, Daresbury, UK, 1991).
25. K. D. Cowtan and P. Main, *Acta Crystallogr. D* **52**, 43 (1996).
26. T. A. Jones, J. Y. Zou, S. W. Cowan, M. Kjeldgaard, *Acta Crystallogr. D* **47**, 110 (1991).
27. A. T. Brunger *et al.*, *Acta Crystallogr. D* **54**, 905 (1998).

28. Supported in part by grants from the National Institutes of Health, The Wellcome Trust, and the Burroughs Wellcome Fund. We thank J. Endrizzi for assistance maintaining our diffraction facilities and offering helpful advice. We thank J. Holton for the use of ELVES, T. Alber and J. Berger for their insights and observations, and T. Earnest and the staff at the Advanced Light Source for their help. We thank T. Handel and her lab for their support, D. Koshland Jr. and S. Marqusee for use of the MCS-ITC instrument, and M. Haggart for DNA sequencing and oligonucleotide synthesis. We thank D. Rio, M. Botchan, and B. W. Matthews for their comments on the manuscript.

2 February 2000; accepted 6 April 2000

Rapid Destruction of Human Cdc25A in Response to DNA Damage

Niels Mailand, Jacob Falck, Claudia Lukas, Randi G. Syljuåsen, Markus Welcker, Jiri Bartek,* Jiri Lukas

To protect genome integrity and ensure survival, eukaryotic cells exposed to genotoxic stress cease proliferating to provide time for DNA repair. Human cells responded to ultraviolet light or ionizing radiation by rapid, ubiquitin- and proteasome-dependent protein degradation of Cdc25A, a phosphatase that is required for progression from G_1 to S phase of the cell cycle. This response involved activated Chk1 protein kinase but not the p53 pathway, and the persisting inhibitory tyrosine phosphorylation of Cdk2 blocked entry into S phase and DNA replication. Overexpression of Cdc25A bypassed this mechanism, leading to enhanced DNA damage and decreased cell survival. These results identify specific degradation of Cdc25A as part of the DNA damage checkpoint mechanism and suggest how Cdc25A overexpression in human cancers might contribute to tumorigenesis.

High-fidelity maintenance of genomic integrity in eukaryotes is ensured by DNA repair and cell cycle checkpoints, surveillance pathways that respond to DNA damage by inhibiting critical cell cycle events (*1*). The key G_1-phase checkpoint in mammalian cells re-

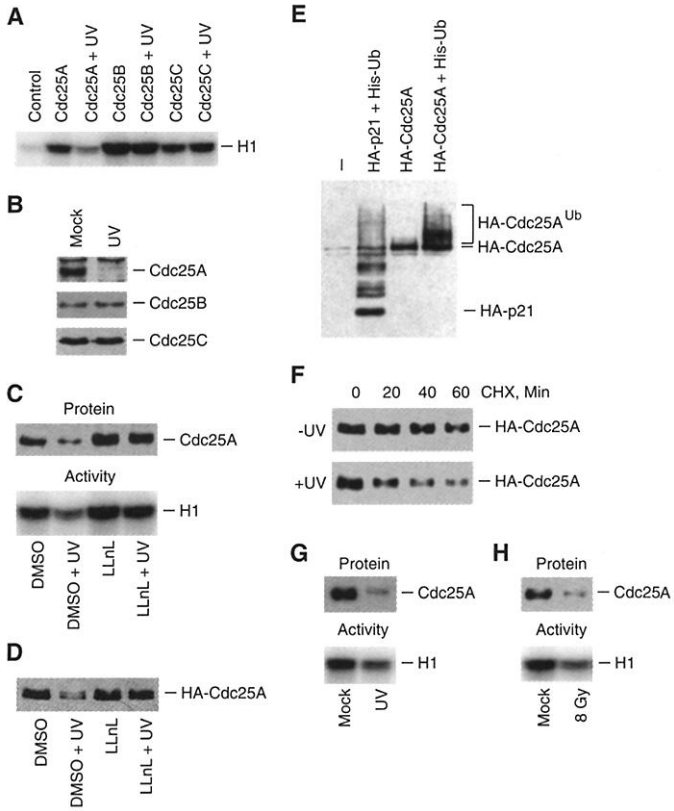

Fig. 1. Proteasome-dependent degradation of Cdc25A in response to DNA damage. (**A**) Inhibition of the activity of Cdc25A but not that of Cdc25B or Cdc25C in cells exposed to UV. Asynchronous U-2-OS cells were harvested 2 hours after UV treatment (15 J/m^2) (*19*) and assayed for phosphatase activities as described (*20*). (**B**) UV-induced decrease in abundance of the Cdc25A protein, revealed by immunoblotting (*21*) of cells treated as in (A). (**C**) Prevention of UV-induced decrease in abundance and activity of Cdc25A by the proteasome inhibitor LLnL. LLnL (25 μg/ml) or dimethyl sulfoxide (DMSO) was added to the culture medium of irradiated (1 hour) or control U-2-OS cells immediately after treatment. Samples were immunoblotted or assayed for phosphatase activity. (**D**) Degradation of ectopic Cdc25A in a proteasome-dependent manner in UV-irradiated U-2-OS/B3C4 cells (*22*). Expression of the transgene was induced for 12 hours, and cells were treated with LLnL as in (C). Immunoblotting with Cdc25A-specific antibody DCS-122 (*21*). (**E**) Ubiquitination of Cdc25A in vivo. U-2-OS cells were transfected with expression plasmids for hemagglutinin (HA)-tagged Cdc25A or p21 (positive control) and six times histidine-tagged ubiquitin (His-Ub). After denaturing cell lysis, the polyubiquitinated species were purified on a Ni^{2+} column, electrophoretically separated, and visualized by immunoblotting with antibody to HA tag (*8*). (**F**) Half-life of Cdc25A protein in U-2-OS/B3C4 cells treated as in (D). Cycloheximide (25 μg/ml) was added to the medium 1 hour after irradiation and cells were collected at the indicated times. HA-Cdc25A was detected by immunoblotting with antibody DCS-122. (**G**) Effect of UV on Cdc25A in human diploid fibroblasts (IMR-90) exposed to UV (15 J/m^2) and assayed by immunoblotting and phosphatase assays 2 hours after irradiation. (**H**) Down-regulation of Cdc25A in response to γ-irradiation. Irradiated (8 Gy) U-2-OS cells (*19*) were harvested after 2 hours and subjected to immunoblotting and Cdc25A phosphatase activity analysis.

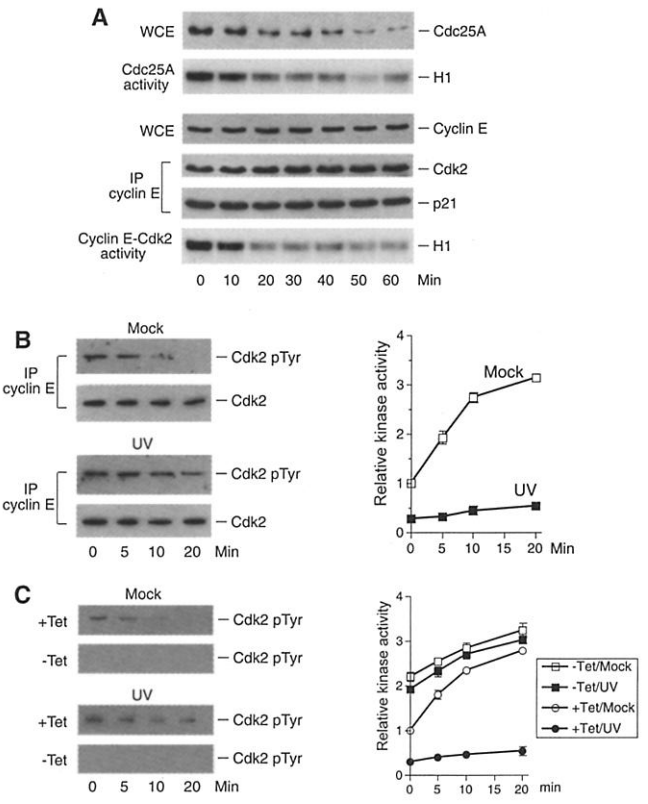

Fig. 2. Effect of UV-induced degradation of Cdc25A on the activity of cyclin E–Cdk2. (**A**) Total amounts of cyclin E and Cdc25A, their associated kinase/phosphatase activities, and association of p21 and Cdk2 with cyclin E in extracts of U-2-OS cells (*20, 21*) harvested at the indicated times after UV irradiation (WCE, whole-cell extracts). (**B**) Rates of tyrosine dephosphorylation and kinase activation of cyclin E–Cdk2 (*10*) are decreased by UV treatment. U-2-OS cells were exposed to UV or left untreated and harvested 1 hour later. Endogenous kinases were inhibited by addition of 10 mM EDTA. Dephosphorylation of Cdk2 was initiated by transferring the lysates from ice to 30°C. At the indicated times, lysates were prepared for immunoprecipitation of cyclin E by immunoblotting with specific antibodies to Tyr^{15}-phosphorylated Cdk2 or total Cdk2 (left). Kinase activity of cyclin E–Cdk2 was measured in an in vitro histone H1 kinase assay (right) (results presented as mean values and standard deviations from three independent experiments). (**C**) Effect of expression of ectopic Cdc25A in U-2-OS/B3C4 (*22*) cells. Tetracycline was removed from the medium 3 hours before UV treatment. Dephosphorylation (left) and kinase activation (right) of Cdk2 were assayed in vitro and data are presented as in (B). Equivalent amounts of Cdk2 were immunoprecipitated from each sample.

lies on the ability of the p53 tumor suppressor to induce transcription of p21$^{CIP1/WAF1}$ (*2*), an inhibitor of cyclin-dependent kinases (Cdks). However, transient inhibition of Cdk2 in response to DNA damage occurs even in cells lacking p53 (*3*) or p21 (*4*). Given the importance of checkpoints for prevention of genetic diseases including cancer, we wanted to explore these alternative mechanisms of G_1 arrest. Because inhibitory tyrosine phosphorylation of the mitotic kinase Cdk1 due to inactivation of the Cdc25C phosphatase underlies the G_2-M checkpoint (*5*), we examined the role of Cdc25 family members, of which at least Cdc25A is essential for entry into S phase (*6*), in checkpoint control of the G_1-S transition.

Exposure of proliferating human U-2-OS osteosarcoma cells (wild type for p53) to ultraviolet light (15 J/m^2) resulted in a rapid decline in phosphatase activity of Cdc25A but not the activities of Cdc25B or Cdc25C (Fig. 1A). This was accompanied by a decline of the Cdc25A but not Cdc25B or Cdc25C proteins (Fig. 1B). Steady-state amounts of Cdc25A mRNA remained unaffected by ultraviolet light (UV) (*7*), whereas treatment

Institute of Cancer Biology, Danish Cancer Society, Strandboulevarden 49, DK-2100 Copenhagen, Denmark.

*To whom correspondence should be addressed. E-mail: bartek@biobase.dk

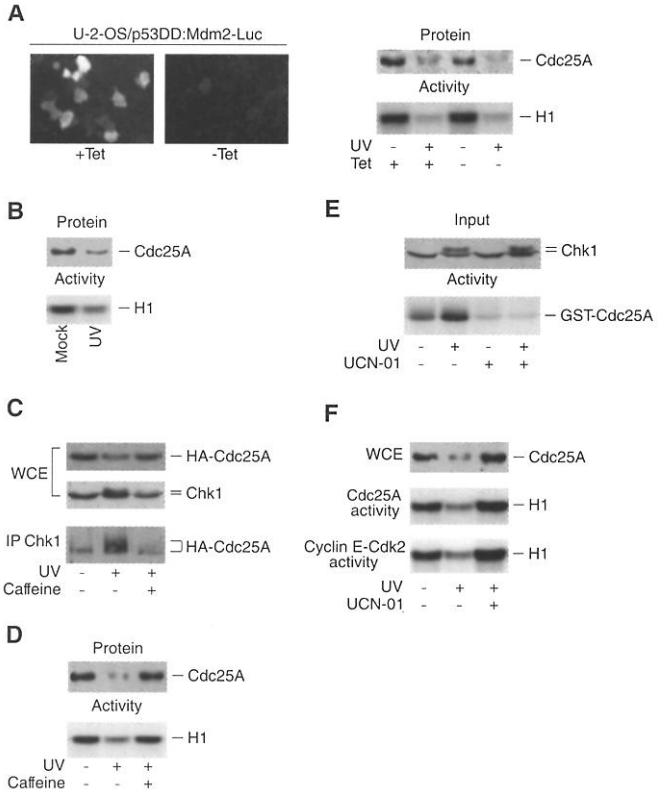

Fig. 3. UV-induced degradation of Cdc25A is p53 independent but requires Chk1. (**A**) Dominant-negative p53 (p53DD) was expressed after removal of tetracycline for 24 hours. p53-dependent transcription in U-2-OS/C6 cells was revealed by immunostaining for luciferase after microinjection of cells with a p53-dependent reporter plasmid (*22*) (left). Cdc25A abundance and activity after 2 hours of UV treatment were determined by immunoblotting and phosphatase activity analyses in cells in which p53DD was not (+Tet) or was (−Tet) induced 24 hours before irradiation (right). (**B**) The Cdc25A response and inhibition of cyclin E–Cdk2 in Saos-2 cells that lack p53. Cells were exposed to UV (15 J/m^2) or left untreated, harvested 2 hours later, and analyzed by immunoblotting and phosphatase/kinase activity measurements (*20, 21*). (**C**) UV-stimulated association of Cdc25A and Chk1. U-2-OS cells were transiently transfected with HA-tagged Cdc25A expression plasmid and either mock-treated, UV-irradiated (15 J/m^2), or UV-irradiated after a 1-hour incubation with caffeine (10 mM). After an additional 2 hours in the constant presence of caffeine, cells were analyzed for levels and complexes of HA-Cdc25A and Chk1 as indicated. (**D**) Effect of caffeine on UV-induced down-regulation of Cdc25A. U-2-OS cells were treated with UV and caffeine as in (C), and Cdc25A protein level and phosphatase activity were analyzed as described (*20, 21*). (**E**) Increased activity of Chk1 toward Cdc25A after treatment of cells with UV. Chk1 was immunoprecipitated from lysates of U-2-OS cells treated as in (B), and its activity was determined in an in vitro kinase assay in the presence or absence of the Chk1 inhibitor UCN-01 (1 μM) (*13*), with purified GST-Cdc25A used as a substrate. An equal amount of Chk1 protein was present in each kinase reaction mixture (Input). Immunoprecipitates obtained with preimmune sera contained only background activity toward GST-Cdc25A regardless of UV treatment (*7*). (**F**) UV-mediated degradation of Cdc25A is prevented by the Chk1 inhibitor UCN-01. Cells were treated and assayed as in (D), except that 300 μM UCN-01 was substituted for caffeine.

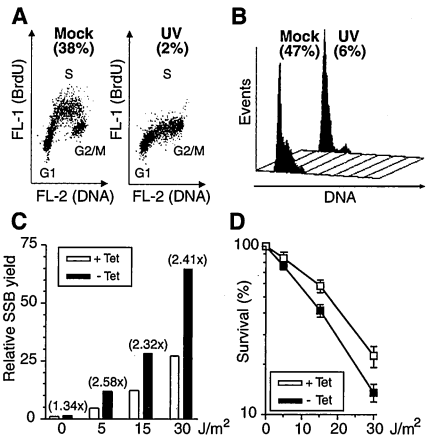

Fig. 4. Effect of UV irradiation on DNA replication, DNA damage, and cell survival. (**A**) Asynchronously growing U-2-OS cells were irradiated with UV (15 J/m^2). Two hours later they were incubated for 10 min with BrdU (100 μg/ml) and analyzed by multivariate flow cytometry (*23*) (FL1-H, BrdU signal revealed by the fluorescein isothiocyanate–conjugated antibody to BrdU; FL2-A, DNA content obtained by counterstaining the cells with propidium iodide). Numbers in parentheses indicate percentages of cells actively synthesizing DNA. (**B**) U-2-OS cells were arrested in mitosis by 12-hour incubation with nocodazole. Eight hours after release, the cells were exposed to UV as in (A) and incubated for another 6 hours before staining with propidium iodide and analysis of DNA content by flow cytometry (*23*). Numbers indicate percentages of cells that entered S phase. (**C**) Increased amount of UV-induced DNA single-strand breaks (SSB) in cells overexpressing Cdc25A. Expression of Cdc25A was transiently induced in U-2-OS/B3C4 cells (*22*) by removal of tetracycline for 3 hours before UV treatment. Thirty minutes after irradiation with the indicated doses of UV and readdition of tetracycline, formation of DNA SSB was measured by alkaline elution, exactly as described in (*14*). (**D**) Colony formation assay performed with U-2-OS/B3C4 cells exposed to the indicated doses of UV light and evaluated 12 days after irradiation. Cdc25A protein was transiently induced (−Tet) as described in (C).

with the proteasome inhibitor LLnL immediately after UV irradiation prevented reduction in the amount of both the endogenous (Fig. 1C) and the ectopic Cdc25A protein expressed from a heterologous promoter (Fig. 1D). In an in vivo protein ubiquitination assay (*8*), we detected abundant species of polyubiquitinated Cdc25A (Fig. 1E), and protein turnover measurements demonstrated shortening of the Cdc25A half-life in U-2-OS cells exposed to UV (Fig. 1F). These experiments showed that Cdc25A is targeted by the ubiquitin-proteasome pathway and that its turnover becomes accelerated in response to UV light.

To explore the possibility that Cdc25A protein stability represents a previously unrecognized target of a checkpoint response to genotoxic stress, we first reproduced the experiments in normal diploid cells. IMR-90 human fibroblasts irradiated with UV showed decreased phosphatase activity of Cdc25A and decreased abundance of the Cdc25A protein (Fig. 1G). We detected an analogous decline of Cdc25A protein abundance and activity in both U-2-OS and IMR-90 cells exposed to ionizing radiation (Fig. 1H) (*7*). Thus, in human cells, DNA damage triggers specific destruction of Cdc25A.

We next identified the cyclin E–Cdk2 kinase as the downstream target of the inactivation of Cdc25A. In time-course experiments with U-2-OS cells, Cdc25A protein and its phosphatase activity declined within 30 min after exposure to UV (Fig. 2A). Cyclin D–associated kinase activity and the amounts of cyclins D and E remained unchanged (Fig. 2A) (*7*), whereas cyclin E–Cdk2 activity declined with dynamics matching those of the UV effects on Cdc25A (Fig. 2A). This inhibition was not attributable to recruitment of p21 into cyclin E–Cdk2 complexes or to decreased interaction of cyclin E with Cdk2 (Fig. 2A). These data indicated that the inhibition of cyclin E–Cdk2 in response to UV could reflect persistent inhibitory phosphorylation on Tyr^{15} within the ATP binding lobe of Cdk2 (*9*).

To test whether the inhibition of Cdk2 was causally linked to the UV-induced destruction of Cdc25A, we measured cyclin E–Cdk2 activity as a function of the extent of the inhibitory tyrosine phosphorylation of Cdk2 (*10*). Whereas extracts of mock-treated cells supported tyrosine dephosphorylation and corresponding activation of cyclin E–Cdk2, such phosphatase activity was largely lost in lysates from cells exposed to UV (Fig. 2B). Expression of Cdc25A in amounts that saturated the cellular capacity to efficiently degrade it (*7*) led to an increase of

cyclin E–Cdk2 activity in nonirradiated cells, and UV treatment did not inhibit dephosphorylation of Cdk2 or cyclin E–Cdk2 activity in such cells (Fig. 2C). A similar, albeit less pronounced, effect was observed when cyclin A–associated kinase activity was assayed (*7*). Collectively, these data directly implicate the reduced activity of Cdc25A in UV-irradiated cells in the enhanced tyrosine phosphorylation and consequent inhibition of Cdk2, a kinase essential for DNA replication.

The p53 protein is a regulator of the G_1 checkpoint (*2*), which raises the possibility that it was also required for DNA damage–induced degradation of Cdc25A. We established a U-2-OS subline conditionally expressing a dominant-negative allele of p53, p53DD (*11*). Expression of p53DD abolished the p53-dependent transcription of a reporter gene (Fig. 3A) and expression of endogenous p53 targets such as p21 (*7*). After UV treatment, both the p53 wild-type and p53DD-expressing cells had decreased amounts and activity of Cdc25A and ceased to replicate DNA to a very similar extent (Fig. 3A) (*7*), consistent with similar dynamics of Cdc25A degradation and cyclin E–Cdk2 inhibition in UV-exposed Saos-2 osteosarcoma cells, which lack p53 (Fig. 3B). Thus, the destruction of Cdc25A in response to UV appears to occur independently of p53-mediated transcription.

Because the G_2 checkpoint pathway includes phosphorylation of Cdc25C by Chk1, a kinase capable of phosphorylating all three members of the Cdc25 family in vitro (*5*), we considered Chk1 as a candidate for also mediating the early effects at G_1-S. Exposure of U-2-OS cells to UV induced a shift (*5*) of the endogenous Chk1 on SDS gels (Fig. 3C). This was accompanied by an increase in the amount of Cdc25A associated with Chk1, an effect prevented by pretreatment of the cells with caffeine (Fig. 3C), a compound that interferes with activation of Chk1 (*12*). Treatment with caffeine before UV irradiation also reduced the shift of the Chk1 protein (Fig. 3C), abolished the destruction and loss of activity of Cdc25A (Fig. 3D), and restored the half-life of the Cdc25A protein to the values measured in nonirradiated cells (*7*). Chk1 kinase assay using glutathione S-transferase (GST)–tagged Cdc25A as a substrate revealed that the activity of Chk1 increased reproducibly in cells exposed to UV (Fig. 3E). Both basal and UV-induced Chk1 activities were inhibited by the Chk1 inhibitor UCN-01 (*13*) (Fig. 3E), and treatment of cells with UCN-01 at the time of UV irradiation abolished the degradation of Cdc25A and allowed maintenance of the activities of both Cdc25A and cyclin E–Cdk2 (Fig. 3F). These data implicate Chk1 as an upstream regulator of Cdc25A degradation after UV-induced DNA damage.

If the Chk1-Cdc25A-Cdk2 pathway indeed represented a bona fide checkpoint response, it would be expected to arrest the cell cycle, and avoiding this response should result in enhanced DNA damage and decreased cell survival. These predictions were tested and confirmed by additional experiments. Brief treatment of proliferating U-2-OS cells with bromodeoxyuridine (BrdU) revealed that ongoing DNA synthesis was inhibited within 1 to 2 hours after UV irradiation (Fig. 4A). Kinetic analysis of G_1-S progression in cells released from nocodazole arrest showed that entry into S phase was also blocked (Fig. 4B). Between 16 and 24 hours after exposure to UV, the cells resumed DNA replication and progression through the cell cycle (*7*), indicating that the UV-induced cell cycle arrest was reversible. An alkaline elution assay (*14*) was then used to measure DNA single-strand breaks that result from uninhibited activity of the DNA replication machinery in UV-damaged cells. Ectopic expression of Cdc25A enhanced formation of DNA single-strand breaks (Fig. 4C), likely resulting from collisions of replication forks with UV-induced DNA crosslinks (*15*). As no DNA strand breaks were induced by ectopic Cdc25A in the absence of UV irradiation (Fig. 4C), the abundance of Cdc25A appears to determine the extent of DNA synthesis upon UV-induced DNA damage. Thus, the elimination of Cdc25A evokes a cell cycle arrest permissive for repair of the DNA crosslinks caused by UV and protects the cells from formation of the DNA strand breaks. Finally, consistent with the third prediction for a checkpoint response, a 3-hour period of expression of Cdc25A to prevent down-regulation of the cellular Cdc25A activity by UV (Figs. 2, B and D, and 4C) reduced the survival of the irradiated cells examined by colony formation assays (Fig. 4D).

Our results uncover a mechanism of cellular defense against genotoxic stress. The salient features of this G_1-S checkpoint are proteasome-dependent destruction of the Cdc25A, independence of the p53-p21 pathway, involvement of Chk1 operating upstream of Cdc25A, and rapid execution of the response. The characteristics of the Chk1-Cdc25A-Cdk2 pathway, and the fact that the p53-p21 axis affects the cell cycle only several hours after UV treatment (*7, 16*), indicate that the checkpoint response to DNA damage occurs in two waves. The Cdc25A-mediated mechanism may contribute to genomic stability by imposing a cell cycle block and preventing excessive damage of the genome before the p53-p21 pathway ensures a more sustained proliferation arrest (*3, 17*). Deregulation of either mechanism may cause genomic instability. The overabundance of Cdc25A found in subsets of aggressive human cancers (*18*) might prevent its timely degradation in response to DNA damage and thus provide a growth advantage through escape from the G_1-S arrest and propagation of genetic abnormalities.

References and Notes

1. L. H. Hartwell and M. B. Kastan, *Science* **266**, 1821 (1994); S. J. Elledge, *Science* **274**, 1664 (1996); K. Nasmyth, *Science* **274**, 1643 (1996); T. Weinert, *Cell* **94**, 555 (1998).
2. L. J. Ko and C. Prives, *Genes Dev.* **10**, 1054 (1996); A. J. Levine, *Cell* **88**, 323 (1997); C. Lengauer, K. W. Kinzler, B. Vogelstein, *Nature* **396**, 643 (1998).
3. J. A. D'Anna, J. G. Valdez, R. C. Habbersett, H. A. Crissman, *Radiat. Res.* **148**, 260 (1997); H. Lee, J. M. Larner, J. L. Hamlin, *Proc. Natl. Acad. Sci. U.S.A.* **94**, 526 (1997); G. Xie *et al.*, *Oncogene* **16**, 721 (1998).
4. J. Brugarolas *et al.*, *Nature* **377**, 552 (1995); C. Deng, P. Zhang, J. W. Harper, S. J. Elledge, P. Leder, *Cell* **82**, 675 (1995).
5. B. Furnari, N. Rhind, P. Russell, *Science* **277**, 1495 (1997); C. Y. Peng *et al.*, *Science* **277**, 1501 (1997); Y. Sanchez *et al.*, *Science* **277**, 1497 (1997); T. Weinert, *Science* **277**, 1450 (1997).
6. S. Jinno *et al.*, *EMBO J.* **13**, 1549 (1994); I. Hoffmann, G. Draetta, E. Karsenti, *EMBO J.* **13**, 4302 (1994); V. Sexl *et al.*, *Oncogene* **18**, 573 (1999).
7. N. Mailand, J. Falck, J. Bartek, J. Lukas, unpublished data.
8. M. Treier, L. M. Staszewski, D. Bohmann, *Cell* **78**, 787 (1994).
9. D. J. Lew and S. Kornbluth, *Curr. Opin. Cell Biol.* **8**, 795 (1996); G. Draetta and J. Eckstein, *Biochim. Biophys. Acta* **1332**, M53 (1997); N. Rhind and P. Russell, *Curr. Opin. Cell Biol.* **10**, 749 (1998).
10. Our assay was as described by Blasina *et al.* [A. Blasina *et al.*, *Curr. Biol.* **9**, 1 (1999)] except for monitoring phosphorylation of Tyr^{15} on Cdk2 instead of Cdk1.
11. E. Shaulian, A. Zauberman, D. Ginsberg, M. Oren, *Mol. Cell Biol.* **12**, 5581 (1992).
12. A. Kumagai, Z. Guo, K. H. Emami, S. X. Wang, W. G. Dunphy, *J. Cell Biol.* **142**, 1559 (1998).
13. J. N. Sarkaria *et al.*, *Cancer Res.* **59**, 4375 (1999). UCN-01 was a gift from R. J. Schultz (Drug Synthesis & Chemistry Branch, National Cancer Institute).
14. DNA single-strand breaks were measured by alkaline elution with H_2O_2-treated L1210 cells as internal standard exactly as described [M. Sehested *et al.*, *Cancer Res.* **58**, 1460 (1998)]. Relative DNA single-strand break yields were calculated with the SAS statistical software package.
15. W. G. Nelson and M. B. Kastan, *Mol. Cell Biol.* **14**, 1815 (1994).
16. X. Lu and D. P. Lane, *Cell* **75**, 765 (1993); R. Y. Poon, M. S. Chau, K. Yamashita, T. Hunter, *Cancer Res* **57**, 5168 (1997); D. A. Freedman and A. J. Levine, *Cancer Res.* **59**, 1 (1999); C. Blattner, A. Sparks, D. Lane, *Mol. Cell Biol.* **19**, 3704 (1999).
17. J. B. Little, *Nature* **146**, 1064 (1968); A. Di Leonardo, S. P. Linke, K. Clarkin, G. M. Wahl, *Genes Dev.* **8**, 2540 (1994).
18. K. Galaktionov *et al.*, *Science* **269**, 1575 (1995); D. Gasparotto *et al.*, *Cancer Res.* **57**, 2366 (1997); W. Wu, Y. H. Fan, B. L. Kemp, G. Walsh, L. Mao, *Cancer Res.* **58**, 4082 (1998).
19. UV-C (254 nm) irradiation was done in a UV Stratalinker 1800 (Stratagene); the ionizing radiation was delivered by x-ray generator (RT100, Philips Medico).
20. Cdc25 phosphatase activity was measured as activation of cyclin B1–Cdc2. U-2-OS cells were treated with doxorubicin (Calbiochem) (0.2 μg/ml) for 24 hours to induce inhibitory phosphorylation of Cdc2 on Thr^{14} and Tyr^{15} [R. Y. C Poon,W. Jiang, H. Toyoshima, T. Hunter, *J. Biol. Chem.* **271**, 132831 (1996)]. Inactive cyclin B1–Cdc2 was immunoprecipitated with antibodies to cyclin B1 (200 μg of cell lysate per reaction). Cdc25 was immunoprecipitated in parallel from 1 mg of cell extracts treated as indicated. The beads from the cyclin B and Cdc25 immunoprecipitates were mixed, incubated in a volume of 50 μl of a phosphatase buffer [20 mM tris-HCl (pH 8.3), 150 mM NaCl, 2 mM EDTA, 0.1% Triton X-100, 5 mM dithiothreitol] at 30°C for 1 hour, and the reaction was stopped by addition of kinase assay buffer. The activity of cyclin B-Cdc2 was assayed

as described [J. Lukas, G. Draetta, J. Bartek, *Eur. J. Biochem.* **207**, 169 (1992)].
21. Mouse monoclonal antibodies to Cdc25A (DCS-122, DCS-124), Cdc25B (DCS-162, DCS-164), and Cdc25C (DCS-193) were generated by standard hybridoma technology. Monoclonal antibody F-6 to Cdc25A was from Santa Cruz and C23420 to cyclin B1 was from Transduction Laboratories. Rabbit antisera to Cdc25A (SC-7157) and Cdc25C (SC-327) were from Santa Cruz Biotechnology, antiserum to Cdk2 Tyr^{15} (219440) was purchased from Calbiochem, and antiserum to Chk1 was provided by S. Elledge. DO-1 monoclonal antibody to human p53 was from Oncogene Science. Mouse monoclonal antibodies 12CA5 to the hemagglutinin epitope, DCS-60 and DCS-61 to p21, 5D4 to cyclin D1 and D2, HE12 and HE172 against cyclin E as well as immunoblotting, immunoprecipitation, immunostaining, and in vitro kinase assays were described [J. Lukas *et al.*, *Genes Dev.* **11**, 1479 (1997); M. Thullberg *et al.*, *Hybridoma* **19**, 63 (2000)].
22. U-2-OS sublines conditionally expressing HA-Cdc25A (U-2-OS/B3C4) or p53DD (U-2-OS/C6) were generated by transfection with the respective transgenes in pBI plasmids as described [J. Lukas, C. Storgaard Sørensen, C. Lukas, E. Santoni-Rugiu, J. Bartek, *Oncogene* **18**, 3930 (1999)]. U-2-OS/C6 cells were microinjected with the Mdm2-Luc reporter plasmid (25 μg/ml) and nonimmune mouse IgG as a microinjection marker. After 18 hours, the cells were fixed and processed for combined anti-mouse immunoglobulin G and anti-luciferase immunostaining as described [J. Lukas *et al.*, *Genes Dev.* **11**, 1479 (1997)].
23. Conditions for single- and multiple-parameter flow cytometry with a FACSCalibur cytometer (Becton Dickinson) and CellQuest and ModFit software were described [J. Lukas *et al.*, *Oncogene* **9**, 2159 (1994)].
24. Supported by grants from the Danish Cancer Society, the Human Frontier Science Program, the Danish Medical Research Council, and the Alfred Benzons Fund. We thank B. Ducommun, S. Elledge, M. Oren, S. Reed, and C. Ward for plasmids and antibodies and R. J. Schultz (Drug Synthesis & Chemistry Branch, NCI) for UCN-01.

28 January 2000; accepted 29 March 2000

Chromatin-Independent Nuclear Envelope Assembly Induced by Ran GTPase in *Xenopus* Egg Extracts

Chuanmao Zhang[1,2] and Paul R. Clarke[1]

The nuclear envelope (NE) forms a controlled boundary between the cytoplasm and the nucleus of eukaryotic cells. To facilitate investigation of mechanisms controlling NE assembly, we developed a cell-free system made from *Xenopus laevis* eggs to study the process in the absence of chromatin. NEs incorporating nuclear pores were assembled around beads coated with the guanosine triphosphatase Ran, forming pseudo-nuclei that actively imported nuclear proteins. NE assembly required the cycling of guanine nucleotides on Ran and was promoted by RCC1, a nucleotide exchange factor recruited to beads by Ran–guanosine diphosphate (Ran-GDP). Thus, concentration of Ran-GDP followed by generation of Ran-GTP is sufficient to induce NE assembly.

The NE controls access to chromatin and plays an important role in the regulation of chromosome duplication and gene expression in eukaryotic cells. In higher eukaryotes, the NE is highly dynamic in the cell cycle, being disassembled on entry into mitosis and reassembled around the segregated daughter chromosomes at telophase. The molecular mechanism of NE assembly is largely unknown, but the process can be studied in a cell-free system made from *Xenopus laevis* eggs (*1*). In this system, NE assembly around chromatin is inhibited by nonhydrolyzable guanosine 5′-triphosphate (GTP) analogues, suggesting the involvement of a GTPase (*2–4*). One candidate is the multifunctional GTPase Ran (*5*), which in *Schizosaccharomyces pombe* plays a role in the maintenance of NE integrity at exit from mitosis (*6*). Disruption of the Ran GTPase cycle by addition of regulators or dominant Ran mutants inhibits the assembly of nuclei competent for DNA replication in *Xenopus* egg extracts (*7–11*) and perturbs NE structure (*10*, *12*). However, disruption of the Ran GTPase cycle also inhibits chromatin decondensation and the establishment of nucleocytoplasmic transport during nuclear assembly (*11*), making it difficult to distinguish any direct role in NE formation.

To examine whether Ran plays a role in NE assembly independently of its effects on chromatin, we added glutathione-Sepharose beads coated with Ran proteins produced as fusions with glutathione-S-transferase (GST) (*13*) to *Xenopus* egg extracts (*14*). These fusion proteins are functional, because they produce identical effects on nuclear transport and microtubule stability as nonfusion proteins (*10*, *11*, *15*). All of the beads coated with wild-type Ran-GDP became surrounded by a continuous membrane detected with the lipophilic dye 3,3′-dihexyloxacarbocyanine (DHCC) after incubation in the extracts (*14*), whereas beads coated with GST (Fig. 1) or the related GTPases Ras or Rab5 (*16*) did not attract any lipid vesicles. Transmission electron microscopy (*17*) showed a complete double membrane crossed by nuclear pore complexes (NPCs) assembled around Ran-GDP beads, confirming that a NE-like structure was formed (Fig. 1C). To examine the protein components of this NE, we retrieved beads from the extracts and stained nuclear pore complex proteins (nucleoporins) using the monoclonal antibody (mAb) 414 (*18*). Ran-GDP strongly promoted the association of nucleoporins, which were stained around the periphery of the beads, consistent with the assembly of NPCs (Fig. 2, A and B). Ran-beads also attracted the major lamin protein present in the extracts, lamin B_3 (Fig. 2, C and D). This protein is actively imported and assembled into a lamina after completion of the envelope during nuclear assembly from chromatin (*1*), suggesting that active protein import occurs into the pseudo-nuclei formed around Ran-beads and that a lamina may be formed.

To confirm that the NE and NPCs formed by Ran-beads were functional, we carried out an import assay using nucleoplasmin, a karyophilic protein containing a nuclear localization signal. Nucleoplasmin was taken up and strongly concentrated in the pseudo-nuclei, but not in control beads (Fig. 2E). In contrast, a fluorescent dextran too large to pass through nuclear pores was excluded from Ran-GDP beads but diffused into control beads (Fig. 4C). To determine if nucleoplasmin was being imported in a regulated manner, we added dominant Ran mutants after the completion of pseudo-nuclear assembly, but before addition of nucleoplasmin. RanQ69L (substitution of glutamine at position 69 by leucine), which is defective in GTP hydrolysis and therefore locked in the GTP-bound form (*19*), inhibits Ran-mediated nuclear protein import by disrupting the assembly of import complexes (*20*). This mutant strongly inhibited nucleoplasmin import into pseudo-nuclei assembled by using beads coated with Ran-GDP (Fig. 2F), even though NEs remained intact (*16*). Nucleoplasmin import was also inhibited by RanT24N (substitution of threonine at position 24 by asparagine), a mutant that is defective in nucleotide binding and probably blocks import by preventing the recycling of import factors (*11*). We therefore conclude that NE assembled around beads coated with Ran-GDP restricts access of macromolecules but permits the active transport of karyophilic proteins by way of the NPCs.

[1]Biomedical Research Centre, University of Dundee, Level 5, Ninewells Hospital and Medical School, Dundee DD1 9SY, Scotland, UK. [2]Department of Cell Biology and Genetics, College of Life Sciences, Peking University, Beijing 100871, China.

E-mail: c.zhang@icrf.icnet.uk and p.clarke@icrf.icnet.uk